SUBMITTED TO APJ
Preprint typeset using LaTeX style emulateapj v. 11/12/01

MESOLENSING: I. HIGH PROBABILITY LENSING WITHOUT LARGE OPTICAL DEPTH

ROSANNE DI STEFANO
Harvard-Smithsonian Center for Astrophysics, 60 Garden Street, Cambridge, MA 02138
Department of Physics and Astronomy, Tufts University, Medford, MA 02155
Submitted to ApJ, 22 April 2005

ABSTRACT

In a variety of astronomical situations, there is a relatively high probability that a single isolated lens will produce a detectable event. The high probability is caused by some combination of a large Einstein angle, fast angular motion, and a dense background field. We refer to high-probability lenses as mesolenses. The mesolensing regime is complementary to the regime in which the optical depth is high, in that it applies to isolated lenses instead of to dense lens fields. Mesolensing is complementary to microlensing, because it is well suited to the study of different lens populations, and also because different observing and analysis strategies are required to optimize the discovery and study of mesolenses. Planetary and stellar masses located within $1-2$ kpc are examples of mesolenses. We show that their presence can be detected against a wide variety of background fields, using distinctive signatures of both time variability and spatial effects. Time signatures can be identical to those of microlensing, but can also include baseline jitter, extreme apparent chromaticity, events well fit by lens models in which several independent sources are simultaneously lensed, and sequences of events. Spatial signatures include astrometric lensing of surface brightness fluctuations, as well as patterns of time variability that sweep across the background field as the lens moves. Wide-field monitoring programs, such as Pan-STARRS and LSST, are well-suited to the study of mesolensing. In addition, high resolution observations of the region behind a known mass traveling across a background field can use lensing effects to measure the lens mass and study its multiplicity.

1. MESOLENSING

Gravitational lensing was first observed by measuring shifts, on the order of an arcsecond, in the apparent positions of distant bright sources, such as stars lensed by the Sun (Dyson, Eddington, & Davidson 1920; Eddington et al. 1919) or quasars lensed by intervening galaxy clusters (Walsh, Carswell, & Weymann 1979). As the angular resolution of telescopes has improved, the spatial effects caused by lensing have helped to probe the mass distributions of intervening large mass distributions.

Even when images cannot be resolved, time variability may provide evidence that lensing has occurred. Lensing of quasars by stars in distant galaxies, e.g., produces image separations on the order of microarcseconds, generally too small to be resolved. Microlensing can be studied, however, by observing time variations in the image fluxes (see Kochanek 2004 and references therein). In fact, because the projected separation between stars in a distant galaxy can be comparable to the size of their Einstein rings, the probability that an individual source is being lensed by an intervening star (i.e., the optical depth) can be close to unity. Furthermore, the high density of lenses is associated with caustic structures that produce distinctive light curve features.

The term “microlensing" is also used to describe lensing by stellar-mass objects located, e.g., in the Halo, deflecting light from stars in neighboring galaxies. Although the image separations are on the order of a milliarcsecond, they are typically not resolved, and it is time variability that provides believable evidence of lensing. The probability that a given microlens in the Halo is producing a detectable event are typically small ($10^{-7}-10^{-5}$). The time signatures associated with the lensing of a single or binary star by a point or binary lens are distinctive. They are difficult to mimic in data sets that span several years (Paczyński 1996).

In this paper we explore an intermediate (“meso") regime, in which an individual isolated mass has a high probability of lensing a background source. The probability that a mass will serve as a lens may be high because the Einstein angle is large, or because the angular motion of the lens is large. Large values of the Einstein angle and large angular motions can also produce measurable spatial effects. Signatures of mesolensing therefore include both spatial and time effects.

The mesolens regime is complementary to the regime in which the optical depth is high. In the latter case, the lens density is large enough to ensure a high probability of lensing. In the mesolensing case, the lensing probability is high because it is likely that, over a relatively short interval of time, the Einstein ring of an individual lens will encompass the positions of sources bright enough to be detectably magnified.

While supermassive BHs in the centers of galaxies, or intermediate-mass BHs in our own Galaxy may serve as high-probability lenses, the concrete examples we will focus on in this paper (Di Stefano 2005a) are nearby stellar-mass objects located within roughly a kpc of Earth, or planet-mass objects somewhat closer to us. The main distinction between these nearby populations and the classical microlens populations is that each mesolens has a higher probability of serving as a lens. The associated light curve profiles of “events" may be identical to or may be radically different from those typically identified with microlensing. Spatial effects directly associated with lensing or with the motion of the lens may also provide independent evidence of lensing. In some cases the radiation from the lens may be directly detectable.

1.1. *Nearby Objects as Mesolenses*

The properties of the local populations of WDs, NSs, and BHs remain mysterious. We know nothing about isolated BHs (but see Mao et al. 2002; Bennett et al. 2004), little about isolated neutron stars (see, e,g., references in Kaspi, Roberts, & Harding 2004), and, although thousands of WDs have been discovered (Należyty & Madej 2004; Kleinman et al. 2004; Luyten 1999; McCook, & Sion 1999), the distribution of WD

masses is not well established. The frequency of double degenerate systems has not been directly measured, nor has the fraction of neutron stars with planets, nor do we know whether WDs have planets. Finally, recent surveys have discovered large populations of brown dwarfs and low-mass stars, particularly in regions containing young stars; complementary studies are important. Fortunately, stars within roughly a kpc of Earth can be discovered through their action as mesolenses, if they are positioned in front of an appropriate stellar background.

If lensing can provide a systematic way to discover and study nearby dark and dim populations, this will be an important step for several areas of astrophysics. We could, e.g., hope to determine the mass distribution for isolated neutron stars; to derive clues to constrain the neutron star equation of state; determine the size and mass distribution of the population of isolated black holes.

Although the obvious application of lensing studies is to lenses that are dark or dim, all stars deflect light. When light from a nearby nuclear-burning star can be masked, its action as a lens can be studied. This means that we can refine mass estimates, and refine the trajectories of all nearby stars. In principle, we can also determine the fraction with planets orbiting at distances of a fraction of an AU to several AU (Di Stefano 2005b).

1.2. *Mesolensing Monitoring Programs*

The discovery of nearby dark and dim objects can be accomplished through monitoring programs. The most familiar type of monitoring is light curve monitoring, which has been used, e.g., to detect microlensing events that might be caused by lenses located in the Galactic Halo. Mesolensing programs can benefit from light curve monitoring, and also from monitoring that is sensitive to spatial effects.

1.2.1. *Light Curve Monitoring*

The idea motivating previous and ongoing microlensing programs is that monitoring may discover lensing events providing evidence that some fraction of Halo dark matter is in the form of MAssive Compact Halo Objects (MACHOs). Crowded source fields are observed regularly, with cadences that vary, but which may be on the order of once per day. To mitigate the effects of blending, image differencing techniques are implemented. Software programs use a set of criteria based on expected event properties to identify possible microlensing events.

While the existence of MACHOs is still not well established, we know for certain that there is a large population of dark and dim objects within 1 kpc of Earth. Some of these can also be found through monitoring programs. Just as in the case of microlensing, the results are optimized through the use of image differencing. When considering detectability issues in this paper and its companion, we will therefore assume that image differencing is being implemented.

In §3 we compute the rate of well-isolated lensing events due to nearby stars, and also consider the characteristics of such events. We find that many mesolensing events are expected to be of shorter duration than most microlensing events. This suggests that more frequent monitoring than is typical for microlensing events may be helpful. We also find that, although a minimum density of source stars is required, mesolensing is more likely than microlensing to be detected across a wider selection of background source fields. Programs designed specifically for the study of nearby stars might therefore choose somewhat different monitoring patterns than those used to date.

Nevertheless, data from previous and ongoing microlensing monitoring programs should contain events caused by nearby lenses. The rate computations of §3 are specialized to specific background source fields in paper II. We will also derive the characteristic features of events caused by nearby stars. We will find that, while some light curves are identical with microlensing light curves, others have different features.

The challenges observers face in order to optimize the identification of mesolensing events in existing data bases are to (1) design software to select all events that could be due to lensing by nearby masses, (2) develop analysis tools to test the hypothesis that individual events are caused by nearby lenses, (3) search existing data bases for possible counterparts to the lens, and (4) coordinate additional mutliwavelength observations, when they seem to be necessary.

By taking these steps, we can identify events in existing data bases caused by nearby lenses. This serves two purposes. First it can significantly advance our knowledge of nearby stellar remnants and low-mass dwarfs. Second, it clarifies the results of searches for MACHOs, by eliminating contamination from events definitely *not* due to dark halo matter. As new monitoring programs come online, the cadence of observations and background fields can be selected to yield further improvements in our ability to detect and identify events due to nearby lenses.

1.2.2. *Monitoring Spatial Variations*

Astrometric effects fall off slowly with distance from the lens. They are inversely proportional to the distance, with ten percent effects occurring at distances of up to $10\,\theta_E$. The Einstein rings associated with nearby lenses can be on the order of hundredths of an arcsecond, instead of milliarcseconds. This brings the detection of astrometric effects associated with lensing into a regime where they are less difficult to detect. In addition, the lens motion can be on the order of a tenth of an arcsecond per year. This means that it may be possible to detect lensing of source stars located within a swath of width $20-40\,\theta_E$ ($\sim 0.3''$) and length $\sim 10''$. At the distance to M31, this region would cover tens of square parsecs and contain dozens of bright stars, and many more stars too dim to be detectably lensed. Even if only a small fraction of stars are subject to astrometric effects significant enough to be detected, the combination of correlated changes following the track of the lens in a regular way over time, may allow lensing to be identified with a high degree of confidence. This possibility is discussed in §4.

1.3. *Mesolensing by Known Masses*

Beyond establishing some population properties, whenever an event is established as having been caused by a nearby lens, additional study can be carried out. This contrasts with the conventional view of microlensing, prevalent when the programs began, that follow-up observations are unlikely to teach us more about the nature of the lens.[1] Follow-up study of a mesolens can help to determine the nature and mass of the lens and to determine if it has companions.

The possibility of detailed study of a single object as it travels across a dense field is not limited to objects discovered through

[1] There are now several examples of follow-up that has been useful; the most detailed information has been derived for MACHO-LMC-5, an event that was caused by a nearby lens which has now been directly detected.

their action as lenses. A small subset of nearby stellar remnants has already been discovered. In fact, we know of thousands of possibly interesting mesolenses located within a kpc of the Earth. These include pulsars, white dwarfs, L-dwarfs and other low-mass stars, brown dwarfs, and extrasolar planetary systems. Any catalogued masses that lie in front of crowded fields have relatively high probabilities of serving as lenses. In work in preparation, we have begun the task of compiling a catalog of high-probability lenses (Li 2003; Li, Pfahl, & Di Stefano 2005). High-probability lenses can be monitored, and observations of mesolensing can measure lens masses and proper motions. Under favorable circumstances, we can discover whether some of these dim systems are binaries, and may also be able to extract a full orbital solution *without using stellar spectra* (Di Stefano & Pfahl 2005).

1.4. *The Source Population*

Once the lens characteristics have been determined, it is also possible to learn more about the stellar density and luminosity function of the source field. This is also true of microlensing events. What mesolensing adds is an addition to the event rate, providing larger numbers of events than would otherwise be predicted and, in cases in which one lens generates a sequence of events, mesolensing allows individual small regions of the source galaxy to be studied in more detail. Furthermore, as discussed in the companion paper (Di Stefano 2005b), the distribution of event durations for background fields (e.g., galaxies) with the same intrinsic properties, provide a measure of the distance to the background fields, while distributions of durations within a single field map changing stellar densities and luminosity functions across the field.

1.5. *Overview of the Paper*

In §2 I discuss the spatial and time scales associated with mesolensing and in §3, the basics of detection. The possibility of detecting spatial variations is discussed in §4. Section 5 is an overview of the prospects for using mesolensing as a tool in astronomy.

2. MESOLENSING REGIMES

2.1. *Large Einstein Rings*

Let M be the mass of the lens, D_L the distance between the observer and lens, D_S the distance between the observer and source plane, $x = D_L/D_S$. If the alignment between the observer, lens, and source is perfect, the image will be a ring with an angular size referred to as the Einstein angle, θ_E.

$$\theta_E = \left[\frac{4GM(1-x)}{c^2 D_L}\right]^{\frac{1}{2}} = 0.01" \left[(1-x)\left(\frac{M}{1.4M_\odot}\right)\left(\frac{100\,\mathrm{pc}}{D_L}\right)\right]^{\frac{1}{2}} \quad (1)$$

2.2. *Source Density*

If N_S is the volume density of source stars, and L_S is the radial extent of the source galaxy, then [2] σ_S is the number of stars per square arcsecond.

$$\sigma_S = \frac{1.43\times10^4}{\Box''}\left(\frac{N_S}{\mathrm{pc}^{-3}}\right)\left(\frac{L_S}{\mathrm{kpc}}\right)\left(\frac{D_S}{D_{M31}}\right)^2, \quad (2)$$

where D_{M31}, the distance to M31 is 780 kpc (Macri et al. 2001).

2.3. *Relative Velocities*

Let v_L represent the transverse velocity of the lens relative to us; $\omega_L = v_L/D_L$.

$$\omega_L = \frac{0.21''}{\mathrm{yr}}\left(\frac{v_L}{100\,\mathrm{kms}^{-1}}\right)\left(\frac{100\mathrm{pc}}{D_L}\right) \quad (3)$$

The Einstein disks of some lenses traverse enough area in the course of a year to encompass, at one time or another, the positions of many stars. This increases the chance that the lens will pass close enough to the position of a bright star to produce a detectable event.

If the proper motion of the lens is small, the dominant angular motion may be associated with the motion of the Earth. Parallax produces an angular motion of roughly

$$\omega_p = \frac{0.04''\,g}{\mathrm{yr}}\left(\frac{100\mathrm{pc}}{D_L}\right) = \frac{|\mathbf{g(t)}|}{5}\omega_L\left(\frac{100\,\mathrm{kms}^{-1}}{v_L}\right). \quad (4)$$

The average value of the magnitude of $\mathbf{g(t)}$ is determined by the position of the source relative to the ecliptic, and is typically on the order of unity. Both its value and direction relative to the independent transverse motion of the lens vary during the course of a year.

Parallax ensures that the transverse motion of nearby lenses is large enough to allow the Einstein disk to cover the positions of multiple stars during the course of a year, increasing the likelihood of a detectable event. In addition, if a single lens produces a sequence of events, or if the lens can be detected directly, we will be able to track its motion across the source plane; when parallax contributes significantly to the motion, the shape of the lens' track will bear clear and measurable signature of parallax. This will allow us to determine the distance to the lens.

The Sun's motion through the galaxy is associated with an angular motion with respect to sources in a distant galaxy.

$$\omega_S = \frac{6\times10^{-5}\,\mathrm{arcsec}}{\mathrm{yr}}\left(\frac{v_S}{220\mathrm{km\,s}^{-1}}\right)\left(\frac{D_{M31}}{D_S}\right) \quad (5)$$

This is supplemented (or diminished) by a comparable contribution from motion of the source stars within their parent galaxy. Even though this angular speed is relatively small, it can produce interesting effects. For example, if a magnification of 100 is needed to detect an event for which $\theta_E = 0.01''$, an angular speed of $6.2\times10^{-5}\mathrm{arcsec\,yr}^{-1}$ would produce an event lasting 1.7 yrs. If the source stars are located near the center of a galaxy, their speeds can be roughly 10 times as large, and the local source density can be $> 10^6$ pc^{-3}.

2.4. *Mesolensing*

The expressions above demonstrate that there are many situations in which some combination of a large Einstein ring, a dense background field, and large angular motion produces a situation in which an individual mass is likely to lens its background in a way that can be detected during the next year or decade. When an individual lens has a high probability (close

[2] Let z_S represent the radial distance through the source galaxy as measured from the side nearest us. In general $N_S = N(z_S)$, because the source density and absorption may both change change over distances of tens or hundreds of pc.

to unity) that it is producing an event at any given time, or will produce an event in the near future, we will refer to it as a "mesolens". If the position of a mesolens is known, it can be monitored in such a way as to increase the likelihood of detecting its action as a lens, through some combination of light curve and astrometric study. For populations with few known individuals (such as isolated NSs and BHs), monitoring programs can help to discover individual lenses. As we will show below, some features of the required monitoring and analysis are the same as those presently used for microlensing. Others can be optimized by using different strategies. Calculations and predictions must generally take into account the presence of multiple sources in the field of view, more than one of which may be significantly lensed at one time.

2.5. *Stars Entering the Einstein Ring: Rate Per Lens*

We first define the event rate, $\mathcal{R}_1^E$ to be the rate at which source stars enter the Einstein ring of an individual lens. The subscript "1" indicates that this is the rate associated with a single lens; the superscript "E" indicates that this is the rate at which source stars enter the Einstein ring of the lens. With this definition, we can compute $\mathcal{R}_1^E = \mathcal{R}_1^E(M, v_L, D_L; N_S, L_S, D_S)$, the rate of events associated with a single lens of mass M and transverse velocity v_L, located a distance D_L from us, if it is moving in front of a population of source stars D_S from us whose surface density is characterized by N_S and L_S.

$$\begin{aligned}\mathcal{R}_1^E &= 2\,\theta_E\,\omega_L\,\sigma_S \\ &= \frac{60}{\mathrm{yr}}\,\left|\frac{\mathbf{v_L}}{100\,\mathrm{kms}^{-1}} + \frac{\mathbf{g(t)}}{5}\right|\,\left(\frac{N_S}{\mathrm{pc}^{-3}}\right)\left(\frac{L_S}{\mathrm{kpc}}\right) \\ &\times \left(\frac{M}{1.4\,M_\odot}\right)^{\frac{1}{2}}\left(\frac{100\,\mathrm{pc}}{D_L}\right)^{\frac{3}{2}} \\ &\times \left(\frac{D_S}{D_{M31}}\right)^2\left(1-x\right)^{\frac{1}{2}}\end{aligned} \tag{6}$$

The expression above includes the effects of parallax; the vertical bars enclosing the vector sum represent the magnitude of the vector. As the expression indicates, the overall effect of parallax is an increase in path length, producing a proportionately higher rate. As the relative contribution of the transverse component of the velocity decreases, parallax effects will significantly influence the shape of the light curve. An interesting limit is reached when the independent transverse speed is zero, and all events are simply due to the Earth's motion; events will repeat in a manner that depends on the position of the lens. In fact, depending on the distribution of spatial velocities and orientations, a small fraction of all lenses will have their transverse motion dominated by parallax.

Note that, for the parameter values used for normalization, $\mathcal{R}_1^E$ is larger than the number of Einstein diameters per year covered by the lens. This is because, at any given time, more than one source star can be within the Einstein ring. Yet, only a fraction of all of these lensed stars will be bright enough that they can produce an event when the lens approaches at a distance of $\sim \theta_E$.

Astrometric effects can also be important, especially since the size of shifts in image position fall off slowly with distance from the lens. For example, the rate, $\mathcal{R}_1^{10\,E}$, at which stars enter a swath within $10\,\theta_E$ of the lens is ten times larger than $\mathcal{R}_1^E$, and shifts of 10% in the position of positive parity images occur at $\theta = 10\,\theta_E$. Although in many cases astrometric shifts will be difficult or impossible to measure, in others they can help to verify that light curve effects are due to lensing. In still others, astrometry may provide the first hint that lensing is occurring against the background of a distant stellar field.

2.6. *Event Durations*

Define τ_E to be the time taken for the source to pass across the Einstein ring of a lens.

$$\begin{aligned}\tau_E &= \frac{2\,\theta_E}{\omega} \\ &= 35\mathrm{days}\left(\frac{M}{1.4\,M_\odot}\right)^{\frac{1}{2}}\left(\frac{100\,\mathrm{km\,s}^{-1}}{v_T}\right)\left[\frac{D_L}{100\,\mathrm{pc}}(1-x)\right]^{\frac{1}{2}}\end{aligned} \tag{7}$$

For nearby lenses, the time duration increases with D_L, reaching 111 days for a lens at 1 kpc, when all of the other parameters are held at the values chosen above. The value of τ_E continues to increase until $D_L = D_S/2$, and then decreases symmetrically. Thus, if the distributions of lens masses and velocities within the source population are comparable to those found within roughly a kpc of Earth, the range of event durations due to nearby lenses would be similar to that due to self-lensing of the source population.

The Earth's motion can naturally affect the value of τ_E. The duration of short events will shrink or stretch according to the instantaneous relative direction between the transverse velocity, $\mathbf{v_L}$, and $\mathbf{g(t)}$. For events with durations close a year, the duration will not be much affected, but the effect of accelerations is to alter the light curve shape.

2.7. *Total Rate at which Stars Enter the Einstein Ring*

The *total rate* of mesolensing is the rate at which stars in the source galaxy enter the Einstein rings associated with *all* intervening high-probability lenses. Its value depends on the spatial and velocity distribution of lenses. Let $f(M, v_l, D_l)$ represent this distribution, with

$$n_L = 4\pi \int_0^{D_L^{max}} dD_L D_L^2 \int_0^{v_l^{max}} dv_L \int_{M_{min}}^{M_{max}} dM\, f(M, v_L, D_L) \tag{8}$$

where n_L is the number of lenses located within a distance D_L^{max} of us.

We introduce Ω_{gal}, the solid angle covered by the source galaxy, expressed in units of square degrees.

Using the rate per lens, $\mathcal{R}_1^E$ from above, the total rate for an individual galaxy is

$$\begin{aligned}\mathcal{R}_{tot}^E = &\frac{4\pi}{4.125\times 10^4}\,\frac{\Omega_{gal}}{\square^0} \\ &\times \int_0^{D_L^{max}} dD_L D_L^2 \\ &\times \int_0^{v_l^{max}} dv_L \\ &\times \int_{M_{min}}^{M_{max}} dM\end{aligned}$$

(9)

$$\times f(M,v_L,D_L)\mathcal{R}_1^E(M,v_L,D_L;N,L,D_S) \quad (10)$$

To derive some general results we make simplifying assumptions about the form of $f(M,v_L,D_L)$.

$$f(M,v_L,D_L) = \delta(M-\tilde{M})\,\delta(\mathbf{v_L}-\tilde{\mathbf{v}}_\mathbf{L})\,N_L(D_L) \quad (11)$$

The δ–function form for the lens mass roughly corresponds to considering different types of lenses separately. It makes sense, for example, to consider WDs separately from NSs or BHs, since the spatial density of lenses is different for each type of stellar remnant.

If we consider a fixed value for N_L, and consider nearby lenses, so that $D_L << D_S$, then

$$\mathcal{R}_{tot}^E = \frac{3.8\times10^5}{\mathrm{yr}}\frac{\Omega_{gal}}{\Box^o}\frac{N_L}{\mathrm{pc}^{-3}}\frac{N_S}{\mathrm{pc}^{-3}}\frac{L_S}{\mathrm{kpc}}\left(\frac{D_S}{D_{M31}}\right)^2\times \left|\frac{\tilde{\mathbf{v}}_\mathbf{L}}{100\,\mathrm{km/s}}+\frac{\mathbf{g(t)}}{5}\right|\left(\frac{\tilde{M}}{1.4M_\odot}\right)^{\frac{1}{2}}\left(\frac{D_L^{max}}{\mathrm{kpc}}\right)^{\frac{3}{2}} \quad (12)$$

The rate of detectable events is smaller.

3. DETECTING MESOLENSING

When a mass lies in front of a dense source field, a pattern of perturbations in the light distribution is created. The surface brightness fluctuations that would have been observed had the deflecting mass not been there, are redistributed. When the mass travels across the face of the field, the pattern of perturbations changes and moves, introducing time variations that travel across the source field.

Some characteristics of the expected perturbations are the following. (1) They should move in a smooth progression along a well-defined path. (2) For each region in which perturbations are observed, there should be a baseline to which the light received per unit time returns. Time variability occurring before or after the lens passes should be be traceable to the ordinary variability of stars in the region. Other observed variability may be caused by alignment issues an/or by the relatively slow motion of stars in the source galaxy into and out of the region.

Because lensing preserves surface brightness, we should be able to verify that the surface brightness is constant when (3) averaged over space at any one time, and (4) averaged over time in any one region.

If angular resolution on angular scales comparable to θ_E is available, the distribution of surface density fluctuations can be at least roughly tested against lensing model predictions. As a point lens moves across the field, a small disk with relatively steady emission will surround the lens position, traveling with the lens in a way that can be compared to the calm in the eye of a hurricane. A region of more pronounced fluctuations will trace the moving Einstein ring. Even if the angular resolution is significantly worse, however, high-amplification events are expected and can be fit by simple physical models to verify the hypothesis that the observed perturbations are due to mesolensing.

3.1. *The Significant Angular Scales*

Four angular scales determine the characteristics of the signatures of lensing. The first is the Einstein angle, given by Eq. (1). The value of θ_E depends on the mass and position of the lens. For nearby lenses, $x = D_L/D_S << 1$, so the distance to the background source field doesn't play a significant role.

The second scale is θ_1, the angle which encloses, on average, a single source star. The value of θ_1 is determined by the surface density of source stars.

$$\theta_1 = \sqrt{\frac{1}{\pi\sigma}} = 4.7\times10^{-3}\,''\left(\frac{10^3\,\mathrm{pc}^{-3}}{N_S}\frac{\mathrm{kpc}}{L_S}\right)^{\frac{1}{2}}\left(\frac{D_{M31}}{D_S}\right) \quad (13)$$

The third scale is the angle being monitored by our detectors, θ_{mon}. The resolution of the telescope being used for monitoring places a lower limit on θ_{mon}. The number of stars monitored is

$$N_{mon} = \sigma\,\theta_{mon}^2, \quad (14)$$

where we assume that the region monitored is a square with side θ_{mon}.

The fourth relevant scale is set by the value of $\theta_{b,i}$, the angle of closest approach between lens and source required in order for the source by itself to be sufficiently magnified to produce a detectable deviation above baseline. If the lensed source star is bright, contributing most of the light from the monitored region, the value of $\theta_{b,i}$ can be equal to θ_E, or even somewhat larger. In general, however, $\theta_{b,i} < \theta_E$. It is often convenient to use the dimensionless quantity $b_i = \theta_{b,i}/\theta_E$.

3.2. *The Monitored Field*

The total baseline luminosity is

$$L_0 = \sum_{i=1}^{N_{mon}} L_i, \quad (15)$$

where L_i is proportional to the number of photons we receive from the ith star in the monitored region if there is no lensing. In the case of mesolensing, more than one star at a time may be significantly magnified. The total luminosity from the monitored region at time t is therefore

$$L(t) = \sum_{i=i}^{N_{images}} A_i(t)L_i = A_T(t)\,L_0 = \left(1+f_T(t)\right)L_0 \quad (16)$$

N_{images} is the number of images in the monitored region. $A_T(t)$ is the total magnification, and $f_T(t)$ is the fractional change in photons received from the monitored field.

Detectability is defined by a threshold value of $f_T(t)$. The required threshold depends on the physical situation. If the source density is high enough that hundreds of stars lie in the monitored region, then, when we return to the view the same area time after time, small misalignments will mean that a handful of stars could be added in some views, but not others. This can lead to apparent variations on the order of a percent or more. Stellar variability can produce comparable effects. Thus we expect that $f_T(t)$ must typically be at least 0.1, in line with the characteristics of published microlensing candidates observed in M31 (e.g., Paulin-Henriksson et al. 2003). In fact, the successful observations of lensing in M31 illustrate that it is possible to meet the challenge of detecting a lensing event or events against background light, which may itself be fluctuating because of ordinary stellar variability. These observations have used image differencing, which has become standard procedure in microlensing observations, and have identified several good microlensing candidates (Paulin-Henriksson et al. 2003; de Jong et al. 2004).

The value of N_{images} is different from that of N_{mon}, the number of source stars with positions in the monitored region. Every star in the source galaxy contributes a "negative parity" image;

this image is located within the Einstein ring and is highly demagnified ($A << 1$), producing arbitrarily small luminosities as the transverse distance between the lens and source increases. The images that are the most highly magnified are are those associated with stars close to the projected position of the lens. These high-magnification images are located near the critical curves. If the lens is a point mass, the critical curve is a circle with angular radius equal to θ_E.

In the extreme case in which the source field is so dense that it can be viewed as a continuous screen of light, lensing cannot be detected. The magnification of sources very near to the lens or to any associated caustic structures will enhance the amount of light received from these stars, but the associated increase in area will push stars out of the monitored region, eliminating an equal amount of light. Surface density fluctuations can, however, be detectably lensed. Mesolensing therefore spans the regime between the relatively straightforward detection of lensing of a single star, to the undetectable lensing of a uniform region.

3.3. *Detectable Events*

We will focus on the case in which an observable deviation from baseline is due to the lensing of a small number of stars. The same general considerations are necessary to study "pixel lensing" (see, e.g., Gould 1996). Because we are monitoring a region larger than the Einstein ring, all of the positive and negative parity images of stars close to the lens are located in the monitored region. Since, by assumption, these play the major role, we can compute the main features of the expected signatures by considering only stars located in the monitored region, and including the magnification of only the n stars closest to the lens at a given time.

$$L(t) = \sum_{i=1}^{n} A_i(t) L_i + \sum_{i=n+1}^{N} L_i \tag{17}$$

Defining f_i to be the fractional change in light received from the ith source,

$$\sum_{i=1}^{n} f_i(t) L_i = \Big[f_T(t) \Big] L_0. \tag{18}$$

3.3.1. *Approximate Rate*

For large magnification events, $f_i \sim A_i \sim 1/b_i$. Consider the case in which the dominant contribution to the magnification comes from a single star, with luminosity L_i. In order for the total luminosity to increase by an overall factor f_T, this star must come within

$$b_i = \frac{L_i}{f_T L_0}, \tag{19}$$

of the lens. The size of the monitored region must be large enough that L_0 is not zero, so that the value of b_i is well defined.

L_0 can be written as a product of the average luminosity of source stars in the monitored region, $\langle L \rangle$, times the number, N_{mon} of stars in the same region. Thus

$$b_i = \frac{L_i}{\langle L \rangle} \frac{1}{f_T N_{mon}} \tag{20}$$

The rate of detectable single-lens events is

$$\mathcal{R}_1^{detect} = \frac{2\,\theta_E\,\omega\,\sigma}{f_T N_{mon}} \int_{L_{min}}^{L_{max}} dL\, f(L) \frac{L}{\langle L \rangle}, \tag{21}$$

where $\int dL\, f(L) L = \langle L \rangle$, and L_{min} and L_{max} are, respectively, the minimum and maximum source luminosities. Note that this applies to the track of a single lens. If the track is long and covers a wide enough range of luminosities that the integral above is approximately unity, then

$$\begin{aligned} \mathcal{R}_1^{detect} &= \frac{2\,\theta_E\,\omega}{f_T\,\theta_{mon}^2} \\ &= \frac{0.042}{\rm yr} \left(\frac{0.1}{f_T}\right) \left(\frac{1''}{\theta_{mon}}\right)^2 \left| \frac{\hat{\mathbf{v}}_{\mathbf{L}}}{100 {\rm kms}^{-1}} + \frac{\hat{\mathbf{g}}}{5} \right| \\ &\quad \times \left(\frac{M}{1.4 M_\odot}\right)^{\frac{1}{2}} \left(\frac{100{\rm pc}}{D_L}\right)^{\frac{3}{2}} (1-x)^{\frac{1}{2}} \end{aligned} \tag{22}$$

If we know the position of a lens, such as a cool dwarf star or a WD, the chance of detecting a lensing event can be increased by monitoring a smaller area or by using very sensitive photometry.

The total rate of detectable events can now be written as follows, where we assume that $x << 1$.

$$\begin{aligned} \mathcal{R}_{tot}^{detect} = & \\ & \frac{270}{\rm yr} \frac{\Omega_{gal}}{\Box^o} \left(\frac{0.1}{f_T}\right) \left(\frac{1''}{\theta_{mon}}\right)^2 \\ & \left(\frac{N_L}{1{\rm pc}^{-3}}\right) \left| \frac{\hat{\mathbf{v}}_{\mathbf{L}}}{100 {\rm kms}^{-1}} + \frac{\hat{\mathbf{g}}}{5} \right| \\ & \times \left(\frac{M}{1.4 M_\odot}\right)^{\frac{1}{2}} \left(\frac{D_L^{max}}{\rm kpc}\right)^{\frac{3}{2}} \end{aligned} \tag{23}$$

Note that the density of most potential lenses is significantly smaller than 1 pc^{-3}. For WDs, e.g., the value os roughly 10^{-1} pc^{-3} (Holmberg, Oswalt, & Sion 2002; Kawka, Vennes, & Thorstensen 2004; Liebert, Bergeron, & Holberg 2005); the rate per year per square degree is on the order of a few per year. The key to observing a large number of events per year is to survey a large area of the sky.

3.4. *Background Independence*

The above expressions for the rate of *detectable* events are remarkable because they have no direct dependence on the source density. This is because, although a higher source density promotes a higher event rate, the required distance of closest approach is decreased by increasing source density, and the two effects cancel. Nor is there direct dependence on the distance of the source field, D_S. The implication is that virtually any mass that is either fast-moving or has a large Einstein ring can be detected and studied through its action as a lens of distant objects.

Thus, the variety of possible background fields and lensable sources is incredibly diverse. Galaxy halos can be considered, as can the intracluster media of galaxy clusters. Indeed, the expressions for the rates given above assure that mesolensing will be observed by various wide-angle surveys, such as Pan-STARRS (Chambers et al. 2004) and LSST (Stubbs et al. 2004), now being planned. The ultimate background field will be the cosmic microwave background, when fluctuations on small scales are detectable. For cases in which the surface density of stars is prohibitively high, such as in distant galaxies or in the dense nuclear regions of nearby galaxies, ionization nebulae or even X-ray sources can be considered as potentially lensed sources of light, instead of stars.

3.4.1. *Event Characteristics*

Perhaps the most important measurable characteristic of most events is the duration above baseline, τ_i, equal to $b_i \times \tau_E$. The average duration is $\tau_{avg} = \langle b \rangle \tau_E$. The value of $\langle b \rangle$ is $(f_T N_{mon})^{-1}$. For $f_T \sim 0.1$ and $N_{mon} \sim 100$, $\langle b \rangle \sim 0.1$. Given the shape of typical stellar luminosity functions, a small number of high-L stars have luminosities greater than the average; the lensing of these sources will produce events with durations greater than $\tau_{avg.}$. Typical events will be of shorter duration. For a fixed value of v_L and a fixed value of D_L, the distribution of durations will mirror the luminosity function. Because, however, the volume containing lenses increases with the third power of D_L, the overall distribution of event durations will be markedly less skewed toward short-duration events than the luminosity function is toward low-L stars.

It is nevertheless interesting that, because the integral over luminosities extends to the least luminous stars in the source field, events with durations several orders of magnitude smaller than the average could occur. What determines the shortest duration observable? Analogies with microlensing may suggest that it is finite-source size effects. However, in mesolensing, the projected linear dimensions of the Einstein rings tend to be large. ($0.01''$ corresponds to ~ 8000 AU at the distance to M31.) The limit typically comes, instead, from signal to noise (S/N) requirements. If, e.g., a low-L star is magnified, the value of b_i required for a detectable event may be so small, that τ_i is a minute or less. Even if we happened to be observing the location at which the event is occurring, the value of S/N integrated over an exposure may not be large enough to allow the event to be detected. For any given observational set-up, there is therefore an effective cut-off of the distribution of time durations. Nevertheless, depending on value of τ_E and the luminosity distribution of the source field, some events with durations < 1 day may be detectable.

3.4.2. *Corrections*

Several approximations have been used.

(1) We have assumed that we are monitoring a region in which there are stars that can be detectably lensed. This implies first of all that the baseline luminosity should not be zero. Second, there should be some value of b_i for which an event could, in principle, be detected. All of the unlensed stars should not be so dim, e.g., that the small values of b_i required, produce events too short to be detected.

(2) We have assumed that the deviation is due to the lensing of a single source. While this tends to be the case for the highest magnification regions of the highest magnification events, the simultaneous lensing of several stars contributes to many events. Multiple source events are generally more complex, and have higher duty cycles. They are discussed in §3.5.

(3) We specifically considered events with such high magnifications that $b \sim 1/A$. This is a good approximation for $A > 2$. We should therefore consider separately distances of closest approach larger than roughly 0.5. The only stars that can be detectably magnified for such large values of b are those with

$$L_i > L_{low} = \frac{f_T L(0)}{\frac{b^2+2}{b\sqrt{b^2+4}} - 1} \tag{24}$$

The monitored region can contain at most n such stars, where n is small. For example, with $f_T = 0.1$, and $b \sim 0.5$, $L_{low} > 0.1\,L(0)$; ten or fewer stars can satisfy this condition. To derive an exact expression for $\mathcal{R}_1^{detect}$, we must truncate the luminosity integral in Eq. 21 at $L_{max} = L_{low}$, and add a term for the contribution of more luminous stars. The new term is the integral over luminosities of $2\,b_i\,\theta_E\,\omega_L\,\sigma$, where the value of b_i will range from 0.5 to a maximum that could be as high as ~ 1.7, and the value of σ for these bright stars is n/N_{mon} times the value for all stars. Thus, the functional form of this new term is the same as that of $\mathcal{R}_1^{detect}$ derived above, and, in addition, its value will be close to the value given above. We will therefore continue to use the estimates given in Eqs. 22 and 23. Note, however, that, depending on the luminosity function these estimates can be very close to the rates for bright stars alone.

(4) We have averaged over the source luminosity, which is equivalent to assuming that the portion of the track we are considering is long enough to well-sample the distribution of source luminosities. While this may be appropriate for $\mathcal{R}_{tot}^{detect}$, because many lenses are included, the value of $\mathcal{R}_1^{detect}$ for a specific lens depends on the details of the source field behind that lens. If, therefore, an individual lens is being monitored, both the sampling strategy and predictions can be designed to suit that specific case and to improve the chances of event detection. By using better resolution and more sensitive photometry the rate of events that can be well fit by lensing models can be increased by two orders of magnitude. In addition, measuring spatial effects such as a sequence of perturbations that track the lens, or centroid shifts due to lensing, can provide supplementary information that verifies that lensing is occurring and helps to constrain models.

3.5. *More Complex Perturbations*

Above we considered the limit in which there are well-separated events due to lensing of a single source star. In some cases, however, a sequence of events (i.e., a set of "repeating events"), or even the simultaneous detectable lensing of several sources is expected. These regimes are delineated by the value of θ_1 and its relationship to θ_{mon} and θ_b.

Ultra-low density: When the monitored regions contain, on average, less than a single star, we are in the ultra-low-density regime: $\theta_1 > \theta_{mon}$.

$$\sigma_S < \frac{1}{\pi\,\theta_{mon}^2} \tag{25}$$

In this regime, events involving the simultaneous lensing of more than one star are rare. In addition, blending of light from the lensed source with other monitored sources will not typically be important. The majority of light curves will be generated by individual source systems. Data analysis can proceed as it would in the case of individual microlensing events. The high probability nature of the lensing is expressed only through a high event rate, most likely caused by a fast-moving lens.

3.5.1. *Low, Medium, and High Density*

Consider the case in which $\theta_1 < \theta_{mon}$. Then, the condition that the time between events ($\sim 1/\mathcal{R}_1$), is significantly larger than typical event durations ($2\,\theta_b/\omega$), is

$$4\,\theta_b^2 < \pi\,\theta_1^2 \tag{26}$$

In other words, if we consider a disk of radius θ_b, the probability that it is occupied by a source star must be small.

The part of the parameter space we will refer to as the *low density* regime is $\theta_b << \theta_1$. In the low-density regime, events are distinct and well-separated from each other. They are unlikely to repeat, and will simply be blended versions of Paczński

light curves. The amount of blending is determined by the ratio θ_1/θ_{mon}. The duty cycle is low. The value of θ_b/θ_1 in the top left panel of Figure 1 is 0.018, depicting the low density regime.

As the value of θ_b/θ_1 increases, the duty cycle also increases, and there is a higher probability of detectable "repeats" in the course of a year. The lower panels of Figure 1 illustrate the *medium density* regime, with $\theta_b/\theta_1 = 0.09$ on the lower left, and 0.18 on the lower right. If, as in the figure, the increase in θ_b/θ_1 is due to an increase in the value of θ_b, then event durations also increase in this regime.

As the value of θ_b/θ_1 increases toward unity, the circles of detectability associated with different lenses begin to merge. There are, therefore, not only repeating events, but events of even longer duration. These latter are due to the simultaneous lensing of several source stars. The duty cycle of activity is large in the *high density* regime, shown in the upper right panel of Figure 1, where $\theta_b/\theta_1 = 0.54$.

Note that the terms low-, medium-, and high-density refer to the values of the ratio θ_b/θ_1, and not to the value of θ_1 itself, which characterizes the surface density of source stars. Figure 1 illustrates that, even with a constant surface density, the changes in θ_b that span a factor of 10 can span the low- to high-density regimes.

Table 1 applies to the same situation, illustrating how the duty cycle and event characteristics change with increasing values of θ_b/θ_1.

In more realistic situations, the source stars will span a large range of luminosities. The circle of observability around different stars will have radii equal to $\theta_{b_i} \sim L_i/\langle L\rangle$. The bright stars will therefore have the highest probability of being part of a sequence of events; events involving bright stars are the events most likely to deviate from the simple Paczyński form.

3.5.2. *Model Fits*

By focusing on regions of the light curve with high total magnification, we can effectively limit consideration to regions with arbitrarily small values of θ_b. This corresponds to entering the low-density regime, where well-separated single-source models provide good fits. As we include lower-magnification portions of the light curve, the appropriate models depend on the intrinsic source density. If it is high, then acceptable fits may require multiple-source models. This is demonstrated in the companion paper.

4. SPATIAL EFFECTS

During lensing there are shifts in the number of images, their positions, and in the surface area of each. The light curve calculations carried out for the simulations in paper II include all of these effects. The high-magnification portions of the light curves are, however, dominated by changes in area of individual images. These magnification effects fall off rapidly with distance.

$$A(u) - 1 \sim \frac{1}{u^4} \tag{27}$$

Astrometric effects fall off less rapidly ($\sim \frac{1}{u}$), hence can in principle be detected in a larger area around the lens. With significant deviations occurring over a larger area, they also apply to a larger number of source stars. In Figure 2, I show the changes in image positions of stars in a region that is $20\,\theta_E$ on a side, centered on the lens position. The source density is $1/\theta_E^2$. The source positions (black crosses) were generated randomly. Red crosses mark the positions of the positive parity images.If u is the projected distance between the source and lens, and u_+ s the projected distance between the positive parity image and lens, then

$$d_+ = u_+ - u \sim \frac{1}{u} \tag{28}$$

The overall effect, which can be seen in Figure 2, is a differential stretching of the locations of positive partity images. Equally important, the location of the lens is moving, so that each region traversed by the lens experiences the stretching and then relaxes back to its original shape, while the perturbation moves on to the next region.

The detectability of astrometric effects has been studied in a number of different situations. The case of a large, static Einstein ring projected against M31 and observed by *HST* was considered by Turner, Wardle, & Schneider (1990). Pattern magnifications were considered by Saslaw, Narasimha, & Chitre (1985). On the other extreme, astrometric effects acting on individual stars have also been considered (see, e.g., Paczýnski 1996b; Dominik & Sahu 2000; Jiang et al. 2004).

One significant feature of mesolensing by nearby stars is that the size of the Einstein rings tend to be larger than in microlensing. This means that larger astrometric shifts are expected, and can be more easily measured. Another important characteristic is that angular speeds tend to be high. Against a dense background field, many stars may therefore come within roughly $10-20\,\theta_E$ of the lens during a time interval of years. The large numbers of shifts expected, in a population of stars likely to exhibit surface density fluctuations, mean that lensing effects can in principle be observed with a high level of confidence. Estimates are made by Propotopapas et al. (2006).

In many mesolensing situations, it will not be possible to detect for an individual star, the apparent image motion caused by lensing. Nor will the Einstein radius generally be large enough to resolve the Einstein ring and study the sorts of effects considered by Turner, Wardle, & Schneider (1990). Nevertheless, the number of stars per year that come within $10\,\theta_E$ of the lens is ten times the rate $\mathcal{R}_1^E$. The number of stars in a $20\,\theta_E$ swath covered by an individual lens per year may therefore be large enough that it encloses a significant number of surface brightness fluctuations. (In some cases, nebulae may be included as well.) It may be possible to detect slight deviations in the shapes and positions of these as the lens approaches and then departs. Because the lensing model has few free parameters, and there may be many individual motions to study, there should be cases in which it is possible to verify the lensing model through studying the time and spatial evolution of a large number of slight shifts. Such studies would have much in common with studies of weak lensing in the cosmological context, although time variability of the signal would provide additional useful information.

5. CONCLUSION

5.1. *Summary*

Mesolensing is high-probability lensing. The high probability is associated with some combination of a large Einstein ring and fast angular motion. Under a set of simple assumptions, the rate of events in which the total magnification of a monitored field exceeds any given value is independent of the source density. This means that, in principle, the entire sky is a suitable background in which to search for evidence of mesolensing. If, e.g., we could discern small-scale variations in the microwave background (due, possibly, to the Sunyaev-Zeldovich

effect [see, e.g., Springel, White, & Hernquist 2001 and references therein]), the entire sky could be a background against which we can discover and study nearby stars. For now, many stellar backgrounds can be used.

Although the event rate is background-independent, the event characteristics are not. In more dense backgrounds, event durations are shorter, and the duty cycle and incidence of simultaneous multi-source lensing can each be larger. This means that, for identical source fields located at different distances from us, event characteristics can be used as a distance indicator. This method to measure distances uses time variations in a way that is analogous to the use of surface brightness fluctuations (Tonry & Schneider 1988; see also references in Mei et al. 2005). Furthermore, for sources at a fixed distance, the event durations and incidence of multiple-source events, map the source density.

The first goals of mesolensing observations are to discover lenses and, for known lenses, to determine the lens mass. We may also be able to refine measurements of the distance to and angular speed of the lens, and also to study its multiplicity (Di Stefano 2005a). Mesolensing effects are measurable in both the time and space domains. The angular resolution and photometric sensitivity required to optimize the observing strategy will depend on the characteristics of the background.

Time variability can be most easily studied when it produces well-defined events. I have demonstrated that the highest magnification portion of such events is likely to be due to the lensing of a single source and to therefore produce a light curve profile similar to those found in microlensing. When the source density is high (relative to the size of $b_i \theta_E$), the light curve shape near regions of peak magnification can be influenced by the presence of a small number of individual sources. Even then, fits to a simple model should be possible. In the high-density regime, the long-time light curve can be fit by a sequence of events, where the baseline flux may be different at different times, because the lens is passing across different regions of the source field. In low-density regions, most events will have the same characteristics as microlensing events and, although they can repeat, the time between events can be tens or hundreds of years. Therefore, even an event due to a nearby dwarf star or stellar remnant may appear to be a “garden variety" microlensing event. Nevertheless, nearby lenses are more likely to be directly detectable in some waveband and parallax effects may also be discernible.

Spatial variability can provide independent checks of lensing, and can also be used to discover lensing. Spatial variability may be observable due to both the effects of lens motion and to lensing induced shifts in image position as the lens traverses the source plane. The sequential appearance and disappearance of weak-lensing perturbations along the lens track is a possible signature that provides independent information about the size of the Einstein ring.

Overall, the possible combination of both time and spatial effects provides more information with which to test lensing models than is typically available for microlensing events. This can be so even in cases in which direct imaging and spectral studies of the lens are not possible.

5.2. *Prospects*

This paper has introduced the idea of high-probability lensing, or mesolensing. While many of the ideas represent natural extensions of microlensing and macrolensing studies, it is worthwhile to develop a framework specifically suited to high-probability lensing. To use such lensing as an effective tool in astronomy, computations, selection procedures, and even observing procedures need to be designed to study the related effects. High-probability suggests directions for new investigations.

Computation of mesolensing effects take into account the presence of multiple sources that may be lensed by a single mass, either simultaneously or in sequence. The effects can be searched for in the data collected by existing or completed monitoring programs. Modifications of the software to include as candidates monochromatic signals, multiple-source signals, and sequential events with possible jitter in the baseline are needed to optimize the identification of mesolensing candidates. Searches designed specifically to study possible spatial effects may also be important.

Because the effects of a bright background are to require a closer distance of approach for detectability, a subset of mesolensing events are expected to be of short duration (a day or shorter). In addition, fast angular velocities associated with any masses that may be within roughly a pc of the Earth could produce even shorter events. Observing programs that carry out occasional high-frequency monitoring may therefore prove to be useful. Whatever the cadence of the observations, wide-field monitoring programs designed to come online within the next few years will become important pillars of lensing research.

Many events due to high-probability lenses, especially those occurring against low-density backgrounds such as the Magellanic Clouds or the Bulge, will have the same properties as microlensing events. Others, perhaps the majority, will be identified through loosening the conditions used to select microlensing events. In either case, to establish that the event was produced by a nearby lens requires additional investigation. This includes fits to models with multiple sources, sequential events fit to lensing models, observation of spatial effects, and perhaps most important, multiwavelength “follow up" extending from the infrared through the γ-ray. Multiwavelength follow-up should certainly include correlations with known objects and events in existing catalogs. (For example, some NSs may have experienced episodes of γ-ray activity.) New observations may be required to determine whether candidate events can be associated with nearby objects.

The most obvious application of mesolensing is to the study of nearby stars and planets. A much broader range of applications are, however, possible. For example, different sources, such as nebulae and X-ray sources will be well suited for some studies. Perhaps of most immediate interest, is the extension to lens systems that are intrinsically luminous. If light from a nearby star can be blocked, using techniques similar to those planned for attempts at imaging nearby planets, the mass of the star, and the projected separation of and masses of any companions are potentially measurable.

The systematic study of lensing by nearby objects will increase our knowledge of the mass content and characteristics of the region of the Galaxy inhabited by the solar system. We will learn about the masses, multiplicities, and spatial motions of our neighbors. The information obtained about significant numbers of individual dark and dim nearby stellar remnants and dwarf stars can be woven together to increase our knowledge of star formation, stellar evolution, and of the fundamental properties of each class of lens.

Bennett, D. P., et al. 2002, ApJ, 579, 639

Chambers, K. C., & Pan-STARRS 2004, American Astronomical Society Meeting Abstracts, 205,
de Jong, J. T. A., et al. 2004, A& A, 417, 46
Di Stefano 2005a, *Binary and Planet Mesolenses*, in preparation
Di Stefano 2005b, *Mesolensing Explorations of Nearby Masses: From Planets to Black Holes*, submitted to ApJ
Dominik, M., & Sahu, K. C. 2000, ApJ, 534, 213
Drake, A. J., Cook, K. H., & Keller, S. C. 2004, ApJL, 607, L29
Dyson, F.W., Eddington, A.S., & Davidson, C. 1920, Philos. Trans. R. Soc. London, A220, 291
Eddington, A. S., Jeans, J. H., Lodge, O. S., Larmor, J. S., Silberstein, L., Lindemann, F. A., & Jeffreys, H. 1919, MNRAS, 80, 96
Gould, A., Bennett, D. P., & Alves, D. R. 2004, ApJ, 614, 404 LMC-5
Gould, A. 2004, ApJ, 606, 319 LMC-5
Gould, A. 1996, ApJ, 470, 201
412
Holberg, J. B., Oswalt, T. D., & Sion, E. M. 2002, ApJ, 571, 512
Jiang, G., et al. 2004, ApJ, 617, 1307
Kochanek, C. S. 2004, ApJ, 605, 58
Kaspi, V.M., Roberts, M.S.E., Harding, A.K. 2004, to appear in "Compact Stellar X-ray Sources", eds. W.H.G. Lewin and M. van der Klis, Cambridge University Press, astro-ph/0402136.
Kawka, A., Vennes, S., & Thorstensen, J. R. 2004, AJ, 127, 1702 Observations of White Dwarfs in the Solar Neighborhood
Kleinman, S. J., et al. 2004, ApJ, 607, 426
Liebert, J., Bergeron, P., & Holberg, J. B. 2005, ApJS, 156, 47
Luyten, W. J. 1999, VizieR Online Data Catalog, 3070, 0
Macri, L. M., et al. 2001, ApJ, 549, 721
McClintock, J.E. & Remillard, R.A. 2003, to appear in "Compact Stellar X-ray Sources," eds. W.H.G. Lewin and M. van der Klis, Cambridge University Press, astro-ph/0306213
McCook, G. P., & Sion, E. M. 1999, ApJS, 121, 1
Mao, S., et al. 2002, MNRAS, 329, 349
Mei, S., et al. 2005, ApJS, 156, 113
Należyty, M., & Madej, J. 2004, A&A, 420, 507
Nguyen, H. T., Kallivayalil, N., Werner, M. W., Alcock, C., Patten, B. M., & Stern, D. 2004, ApJS, 154, 266
Paczyński, B. 1996, ARAA, 34, 419
Paczyński, B. 1986, ApJ, 304, 1
Paulin-Henriksson, S., et al. 2003, A&A, 405, 15
Protopapas, P. et al. 2005, in preparation.
Saslaw, W. C., Narasimha, D., & Chitre, S. M. 1985, ApJ, 292, 348
Springel, V, White, M., & Hernquist, L 2001, astro-ph0008144v4
Stubbs, C. W., Sweeney, D., Tyson, J. A., & LSST 2004, American Astronomical Society Meeting Abstracts, 205,
Tonry, J. L., & Schneider, D. P. 1988, AJ, 96, 807
Turner, E. L., Wardle, M. J., & Schneider, D. P. 1990, AJ, 100, 146
Udalski et al, 1994, Ap J 436, 103
Uglesich, R. R., Crotts, A. P. S., Baltz, E. A., de Jong, J., Boyle, R. P., & Corbally, C. J. 2004, ApJ, 612, 877
Volonteri, M., Madau, P., & Haardt, F. 2003, ApJ, 593, 661
Walsh, D., Carswell, R. F., & Weymann, R. J. 1979, Nature, 279, 381

Acknowledgements: This work has been in development for a long time and there are many people to thank. First, Tsafrir Kolatt worked with me on a related question almost a decade ago, considering spatial and time variations due to massive BHs in the Halo. Thanks are due to P.L. Schechter and E.L. Turner for discussions of that idea and to the participants of a 1997 Aspen workshop; especially valuable was feedback from members of the AGAPE team, who tested feasibility. Calculations that led to the present conceptualization were begun at IUCAA in 1998. Jason Li, working under the aegis of *RSI* program run by the *Center for Excellence in Education*, participated in checks of this work in 2003 and developed the idea of creating a catalog of high-probability lenses. I especially want to thank Eric Pfahl for his encouragement to pursue this line of investigation, and for technical discussions. Discussions with many others during the past year have also been helpful, especially Charles Alcock, Lorenzo Faccioli, Arti Garg, B. Scott Gaudi, Matthew J. Holman, Nitya Kallivayalil, Kevin L. Luhman, Christopher Night, Brian M. Patten, and Christopher Stubbs. This work was supported in part by NAG5-10705.

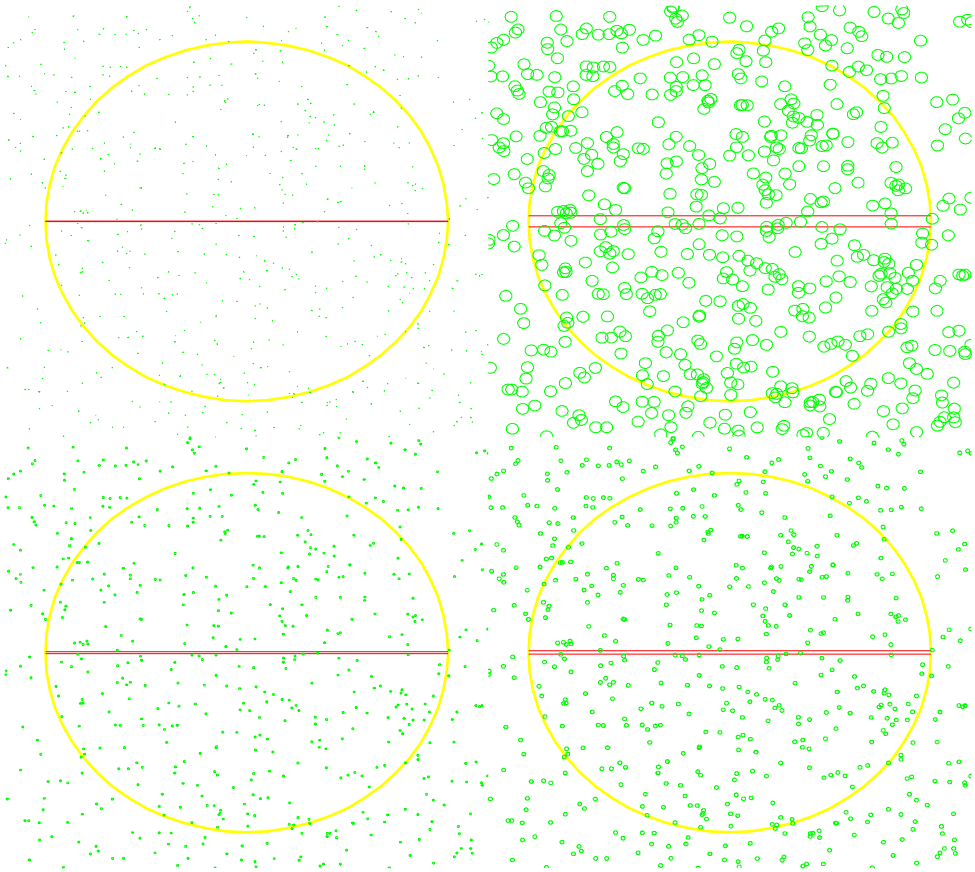

FIG. 1.— The position of each circle represents the randomly-generated position of a source star. The radius of the circle is equal to θ_b, and is the same for all source stars. In these 4 panels, the physical density of source stars has just one value: 1 star/θ_E^2, corresponding to $\theta_1 = 0.56\,\theta_E$. Yet the panels span the range from low density (upper left), counter clockwise to high density (upper right), because the value of θ_b changes from panel to panel. Starting at the upper left panel and moving counter clockwise, $\theta_b = 0.01, 0.05, 0.1, 0.3$. The large yellow circle has a radius of $10\,\theta_E$. the red slice through the center of each panel represents is $2\,\theta_b$ wide and represents the possible track of a lens and the region around it in which source stars can be detectable lensed. If $\omega \sim 20\,\theta_E$ per year, then each red track shows the distance traversed by the lens in a time of approximately one year. For a more realistic luminosity function, there would be a large range of radii, θ_b. Note that in the low-density regime, each event is caused by the lensing of a single source, and that events are well separated; repeats are rare. In the high-density regime, multiple-source events are common and can be of long duration; “repeats" are common and the duty cycle is high.

TABLE 1
PROBABILITY OF MULTIPLE-SOURCE EVENTS

θ_b/θ_1	duty cycle	N_{tot}	P_1	P_2	P_3	P_4	P_5
0.05	0.002	313	0.99	0.00	0.00	0.00	0.00
0.10	0.011	668	0.93	0.06	0.01	0.00	0.00
0.15	0.026	1023	0.82	0.12	0.03	0.01	0.01
0.20	0.054	1465	0.66	0.15	0.06	0.04	0.02
0.25	0.108	2110	0.45	0.16	0.07	0.07	0.07
0.30	0.173	2621	0.34	0.14	0.10	0.10	0.14

Notes: An “event" starts when the lens comes within θ_b of any source and continues as long as the lens is within θ_b of any source; thus events include perturbations due to the simultaneous lensing of multiple stars. The duty cycle is the total time duration of all events occurring during the simulation, divided by the total time of the simulation. N_{tot} is the total number of events. P_i is the fraction of all events in which i source stars were simultaneously magnified during the event (the projected lens position is within θ_b of i stars at some point during the event).

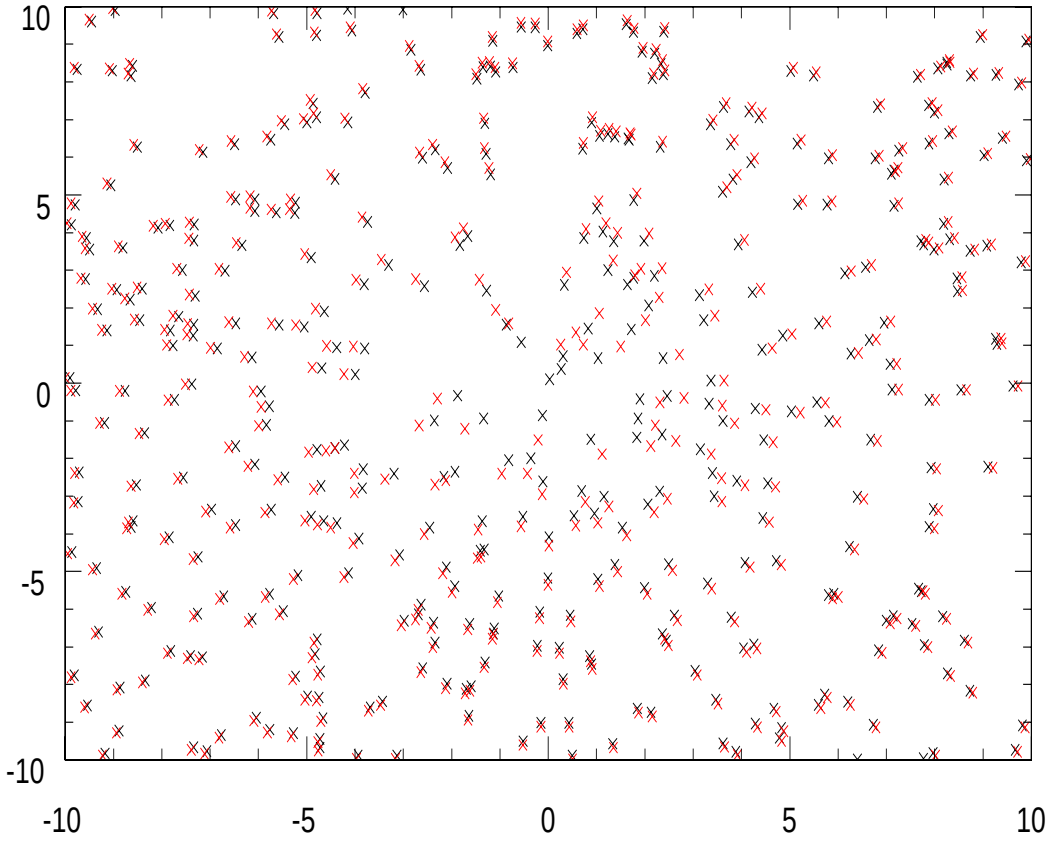

FIG. 2.— Shifts in image position due to a lens located at (0,0); θ_E is the unit of distance along both the vertical and horizontal axes. Black crosses: randomly generated positions of source stars; the source density is 1 per θ_E^2. Red crosses: positions of positive parity images.